ORIGINAL PAPER

# Molecular design of modified polyacrylamide for the salt tolerance

**Lin Yao · Panke Chen · Bin Ding · Jianhui Luo · Bo Jiang · Ge Zhou**

**Abstract** In our work, three kinds of functional monomers were selected to modify polyacrylamide (PAM) or partially hydrolyzed polyacrylamide (HPAM) by molecular dynamics simulation so as to achieve the stronger salt-tolerance of modified HM-HPAM. The radius of gyration ($R_g$), the hydrodynamic radius ($R_H$), the effective length ($L_{ef}$) and the intrinsic viscosity ($[\eta]$) for modified PAM or HPAM were studied in aqueous solutions with different ionic strength at 298 K. The results showed that modified HM-HPAM has a stronger salt tolerance and the salt tolerance increases gradually from HM-HPAM1 to HM-HPAM3 because the monomers with different steric hindrance would reduce the curliness of molecular chains and, consequently, improve the salt tolerance. So, introducing the steric hindrance monomer into polymer will increase the salt tolerance of the polymer and it is indicated that the simulated results agree with the experimental results very well. Furthermore, the radial distribution function (RDF) has been used to investigate the effect of NaCl on the hydration of the –COO⁻ groups of the HM-HPAM from microscopic view.

**Keywords** Hydrodynamic radius · Intrinsic viscosity · Molecular dynamic simulation · Radial distribution function · Salt-tolerance

L. Yao · P. Chen · B. Jiang · G. Zhou (✉)
Key Laboratory of Green Chemistry and Technology, Ministry of Education, College of Chemistry, Sichuan University, Chengdu 610064, China
e-mail: zhougekk@scu.edu.cn

B. Ding · J. Luo
Research Institute of Petroleum Exploration and Development of PetroChina, Beijing 100083, China

## Introduction

Polyacrylamide (PAM) is a very important water-soluble polymer, which is used as a thickener or modifier in the formulations of tertiary oil recovery, drilling fluid, hydraulic fracturing, drag reduction, wastewater treatment [1], paper-making, textile printing, metallurgy, soil improvement and so on because of its structural units with the characteristics of high polarity, high reactivity and easy hydrogen bond formation [2–4]. However, some disadvantages such as poor temperature resistance, pH, salt tolerance and shear capacity limit the application of non-ionic polyacrylamide (PAM) and partially hydrolyzed polyacrylamide (HPAM), especially in petroleum industry [5].

A variety of techniques have been suggested to overcome the problems mentioned above, a series of modified PAM were synthesized [6]. Absolutely, hydrophobically modified polyacrylamide or hydrophobically associating polyacryl-amide, with a small amount (generally molar ratio less than 2 %) of hydrophobic monomer incorporated into the polymer backbone, has received increasing attention on account of its unique rheological characteristics and applications, such as in enhanced oil recovery, drilling fluid, and coating [7–9]. However, the initial concentration of the reaction mixture is relatively low because of gel effect during the course of polymerization, and the water solubility of the hydrophobically associating polyacrylamide is often poor, which makes difficult its practical application [9]. To overcome the limitation, the amphiphilic functional monomers incorporated into the polymer backbone because they were able to greatly enhance the emulsification ability, decrease interfacial tension, and increase the viscosity of the solution and hence allow greater recovery efficiency [5]. As described above, most of the past studies about modified PAM were focused on the traditional experimental methods.

However, to be able to control the rheological properties of such industrially important polymers, it is necessary to understand the aggregation of associating groups at a molecular level [7]. So, molecular dynamics (MD) simulation allows investigators to get a deeper understanding of properties versus different polymer structure. Only a few literature works [10–13] reported the research of the modified PAM solutions by MD. Compared with traditional experimental methods, MD can provide more microscopic information such as the aggregation behaviors and the structures of polymers, surfactants and their mixtures formed at equilibrium, especially for their time development [14]. So, molecular dynamic method is a very useful means for this purpose.

In past research, our research group has studied the different kinds of properties of the PAM and HPAM in aqueous solution from theory (MD simulation) and experimentation [15, 16]. For example, the radius of gyration, the hydrodynamic radius and the ratio of the radius gyration and the hydrodynamic radius, the poor salt tolerance have been studied However, some disadvantages such as the poor salt tolerance need to be further researched at the present stage. The goal of the present work is to improve the salt tolerance of PAM and HPAM. In order to improve the salt tolerance from the theory, we introduce three kinds of monomers into polymer chain (Fig. 1), which are saturated hydrophobic functional moieties. These monomers all possess a benzene ring in side chain. Their structural differences lie in the length of side chain and the number of oxygen atoms in side chain. For these differences, the polymer chain introduced by these monomers exhibited different properties such as the hydrophobicity, the thickening efficiency, the shear-thinning and the salt-tolerance. So the effect of NaCl concentration on the structures of the modified PAM and HPAM were studied by computational method. A theoretical method of MD simulation has been used. A series of hydrophobically modified polyacrylamide (HM-PAM) have been constructed by randomly polymerizing the acrylamide and three kinds of monomers shown in Fig. 1. These polymers were denoted by HM-PAM1/HM-PAM2/HM-PAM3 respectively. With a similar

method, hydrophobically modified partially hydrolytic polyacrylamide (HM-HPAM) has been constructed by randomly polymerizing the acrylamide, hydrolyzed acrylamide and three types of monomers. These polymers were denoted by HM-HPAM1/HM-HPAM2/HM-HPAM3 respectively. Through studying these designed polymers, we hope that the HM-PAM and the HM-HPAM possess the properties such as higher thickening efficiency, stronger shear-thinning and better salt tolerance than conventional water-soluble polymers. Suitable polymer molecules could be selected from designed polymers for further experimental research.

In this work, the dynamic properties of polymer chains such as the radius of gyration ($R_g$), the hydrodynamic radius ($R_H$), the intrinsic viscosity ([$\eta$]) of non-ionic HM-PAM and anionic HM-HPAM in aqueous solutions with different ionic strengths are calculated. Also, more investigations have been focused on the variation tendency of these parameters, which indicate that the influence of the properties of the HM-PAM and HM-HPAM dilute solutions in different ionic strengths by introducing different monomers. At the same time, the radial distribution functions (RDF) between O (−CONH₂) of HM-PAM (or O⁻ (−COO⁻) of HM-HPAM) and H (H₂O) in various NaCl solution models are investigated in hopes of revealing the inherent structure-performance relationship of the dilute modified polyacrylamide solutions.

## Computational methodologies

Molecular dynamics (MD) simulations is a computer simulation technique that allows one to predict the time evolution of a system of interacting particles (e.g., atoms, molecules, granules, etc.) and estimate the relevant physical properties. With the rapid development of molecular dynamics simulation techniques, it is now possible to study the structure and dynamics of biomacromolecular systems in an aqueous environment considering explicit water, ion, and solute molecules [17, 18]. In our work, for all models, construction, minimization, molecular dynamics simulation, and conformational



Fig. 1 Three types of monomer which are used to build modified HM-PAM/HM-HPAM chains

Monomer-1          Monomer-2          Monomer-3
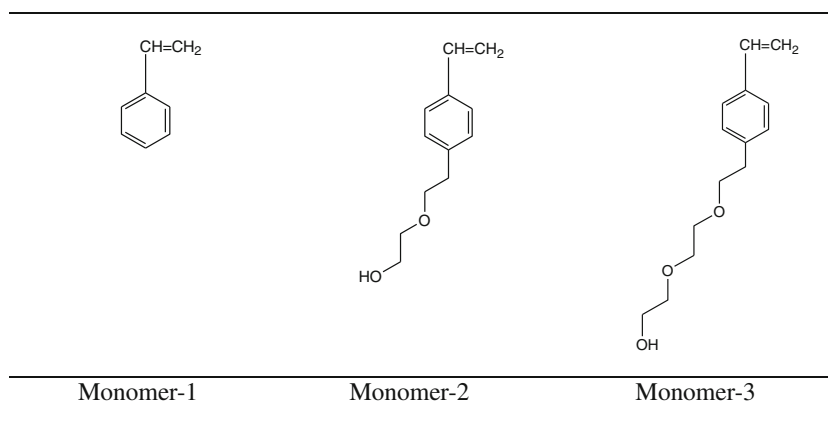
analyses are carried out using Materials Studio program (MS, version 4.2 Accelrys Software Inc., United States). The simulation procedures were as following.

### The construction of HM-PAM and HM-HPAM solution models

The simulations are performed for amorphous unit cells of each investigated polymer with degree of polymerization of 100. Previous researchers have reported reasonable results when they used less monomer for polymer simulation [19–21]. Firstly, the "3D Sketcher" is used to create the three types of monomers (Fig. 1), $H_2O$, $Na^+$, $Cl^-$ and sodium acrylate (NaAA) monomers. The HM-PAM chain (Fig. 2) is constructed using the "Build Polymer" module. The polymer chain consists of 100 repeat units with a 96:4 probability for the occurrence of vinyl-amide unit and various monomers configurations. The HM-HPAM chain (Fig. 2) which consists of 100 repeat units with a 72:24:4 probability for the occurrence of vinyl-amide unit, sodium acrylate unit monomer configurations are built. Reasonable energy minimization was performed for the HM-PAM chain, the HM-HPAM chain, $H_2O$, $Na^+$, and $Cl^-$ using Smart Minimizer method. Next, optimized molecules and ions were embedded into the cubic cells full of 2000 minimized water molecules with 1 g·cm$^{-3}$ density to form all kinds of initial polymer aqueous solution models with different NaCl concentrations, which is constructed by "Amorphous Cell" module. During this process, the period boundary condition (PBC) [22] was taken and a cutoff radius of 10 Å was applied for both non-bonded electrostatic and vander Waals interactions. The solution model is named according to the monomer, for example, the HM-PAM1 means that it contains one polymer chain with a monomer-1 and 2000 $H_2O$ (with a series of different ionic strengths). A part of all models has been shown in Fig. 3. These solutions were submitted to 5000 steps of the smart minimization by the "Discovery" module.

### Simulation details of MD

A 100 ps MD equilibration runs for all the systems that are performed in the NPT ensemble (constants number of particles, pressure, and temperature, $P=1.01\times10^{-5}$ Mpa, $T=298$ K) to obtain the equilibrium density. For MD process, the temperature of the systems was kept through the Andersen [23] method and the pressure of the systems was kept through the Berendsen barostat [24]. An additional 1000 ps NVT (constant number of particles, volume, and temperature $T=298$ K) dynamics is performed on the last frame of the NPT equilibrium stage. The time step was 1.0 fs and the total dynamics time was 1100 ps. All the motion trajectories and coordinate parameters were saved and the frames of the trajectory were output every 10 ps for the subsequent analysis. The non-bond cutoff distance was 10 Å. In all simulations, all calculations are performed
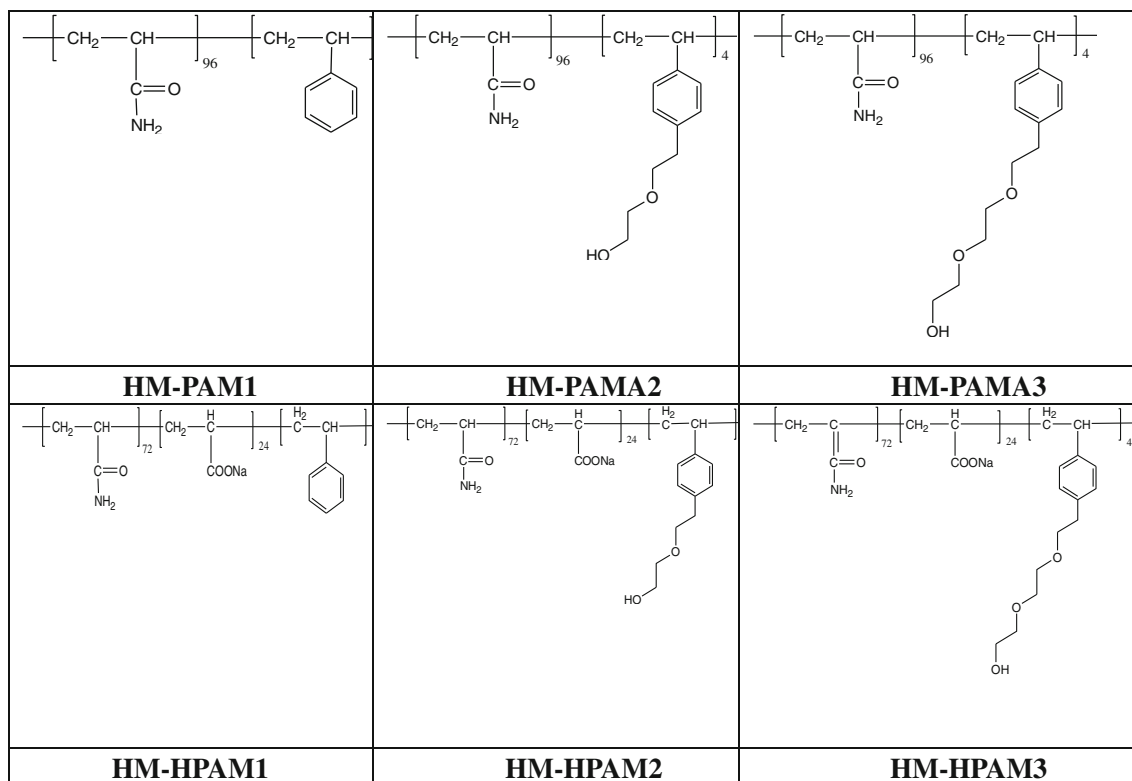


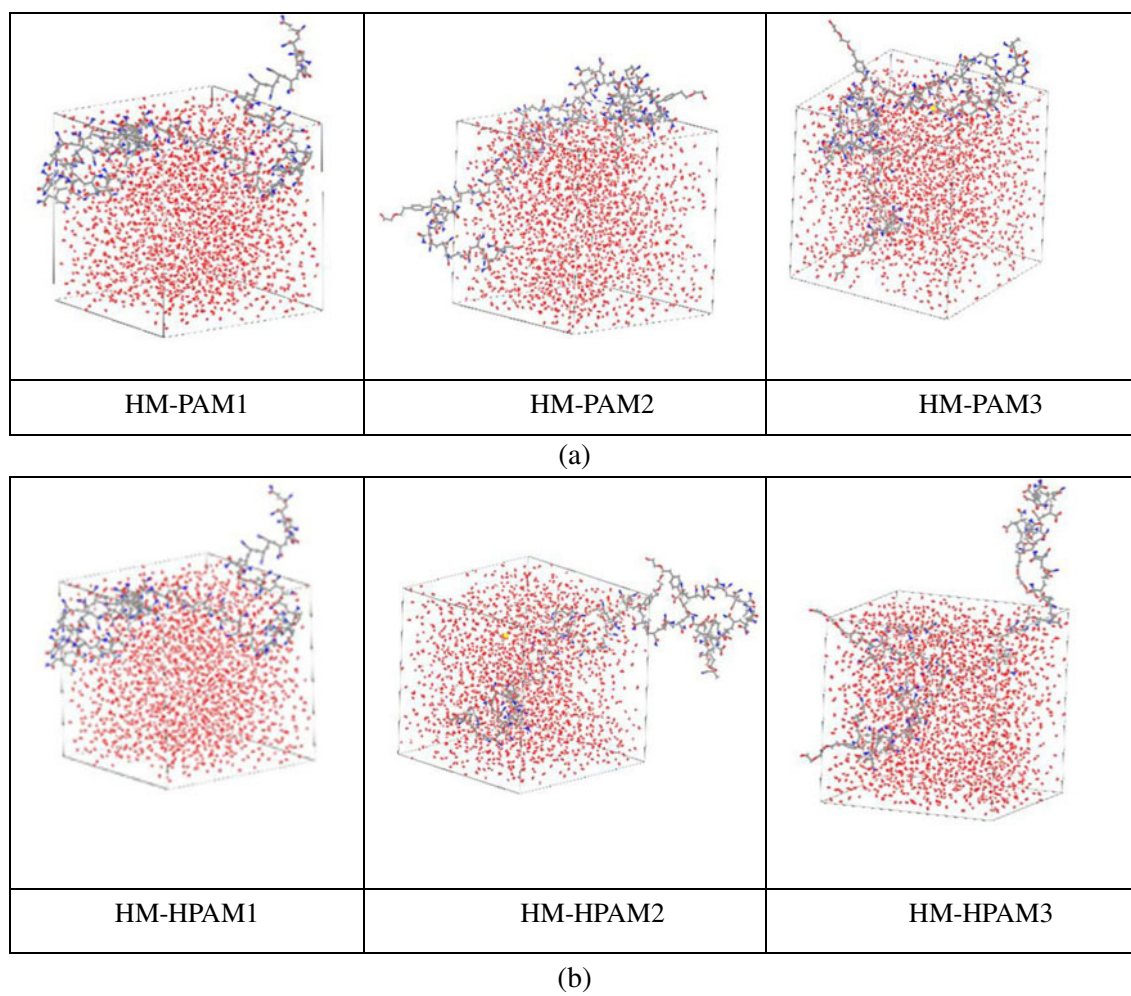**Fig. 2** Structures of a series of designed HM-PAM and HM-HPAM

**Fig. 3** **a** HM-PAM-2000 solution models in the pure water. **b** HM-HPAM-2000 solution models in the pure water

using the PCFF force field. PCFF (polymer consistent force field) is an ab initio forcefield. Most parameters were derived based on ab initio data using a least-squares-fit technique developed by Hagler and co-workers. Many of the nonbond parameters of PCFF, which include atomic partial charges and Lennard-Jones 9–6 (LJ-9-6) parameters were taken from the CFF91 [25–27] force field. The validity of the force field which was used here has already been testified by previous researchers [26, 27]. All force field parameters come from the PCFF force field. So, under a wide range of conditions of temperature and pressure, this force field can guarantee accurate and simultaneous prediction of structural, conformational, vibrational, and thermophysical properties for a broad range of molecules in isolation and in condensed phases.

## Results and discussion

From all simulations above, the mean conformation of every polymer in solution models can be gained as Tables 1, 2 and

3 show. Adamczyk et al. has researched that the hydrodynamic radius ($R_H$) and the intrinsic viscosity ([$\eta$]) for a polymer can be calculated by the parameters ($l$ and $\lambda$) of the molecule shape which is determined by the mean conformation and the equations in Refs [28, 29], for example, for bent spheroid,

$$
\begin{aligned}
&\lambda = l/2b > 1 \\
&R_H = \frac{l}{2\left(\frac{11}{12}ln\lambda - 0.31\right)} \\
&[\eta] = \frac{\lambda^2}{15}\left[\frac{3}{ln(2\lambda)-0.5} + \frac{1}{ln(2\lambda)-1.5}\right] + \frac{8}{5}
\end{aligned}
\tag{1}
$$

$l$ is the extended length and $\lambda$ is the aspect ratio of bare molecule [27, 28].

The mean conformations of every polymer in our solution models take on the bent spheroid as Tables 1, 2 and 3 show. The $R_H$ for the HM-PAM or HM-HPAM molecules and the [$\eta$] can be calculated by Eq. 1 and the parameters of the molecule shape in Tables 1, 2 and 3.

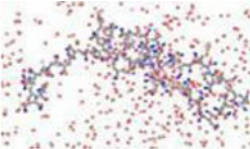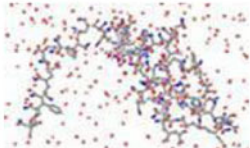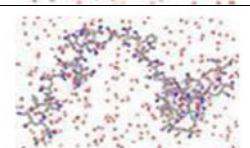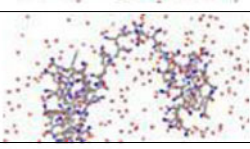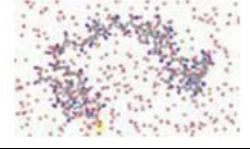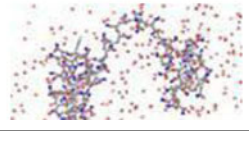**Table 1** Parameters for HM-HPAM1 and HM-PAM1 solution models at 298 K
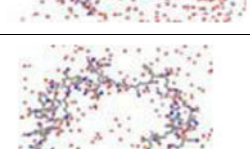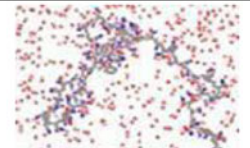
| Solution model | Molecule shape | Snapshot of mean conformation from simulations | $I_{NaCl}$ (mol/kg) | $N_{NaCl}$ | $V_{cell}$ (nm³) | $\rho_{NaCl}(10^{-3})$ (g·cm⁻³) | $\rho_{H2O}$ (g·cm⁻³) | $\rho_P$ (g·cm⁻³) | $L_{ef}$ (nm) | $\Lambda^*$ |
|---|---|---|---|---|---|---|---|---|---|---|
| | | | 0 | 0 | 59.8 | 0 | 1 | 0.2 | 3.5 | 9.2 |
| | | | 0.03 | 1 | 59.8 | 1.6 | 1 | 0.2 | 3.2 | 8.4 |
| HM-HPAM1 | Bent spheroid | | 0.11 | 4 | 59.8 | 6.5 | 1 | 0.2 | 2.7 | 7.1 |
| | | | 0.19 | 7 | 59.8 | 11.4 | 1 | 0.2 | 2.3 | 6.0 |
| | | | 0.28 | 10 | 59.8 | 16.3 | 1 | 0.2 | 2.3 | 6.0 |
| | | | 0 | 0 | 59.8 | 0 | 1 | 0.2 | 2.1 | 4.7 |
| HM-PAM1 | Bent spheroid | | 0.03 | 1 | 59.8 | 1.6 | 1 | 0.2 | 2.0 | 4.8 |
| | | | 0.11 | 4 | 59.8 | 6.5 | 1 | 0.2 | 2.0 | 4.5 |
| | | | 0.19 | 7 | 59.8 | 11.4 | 1 | 0.2 | 1.9 | 4.3 |
| | | | 0.28 | 10 | 59.8 | 16.5 | 1 | 0.2 | 1.9 | 4.3 |

**Table 2** Parameters for HM-HPAM2 and HM-PAM2 solution models at 298 K
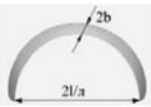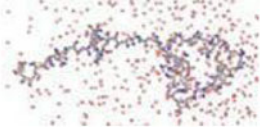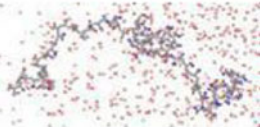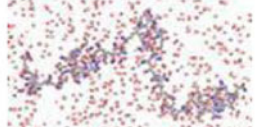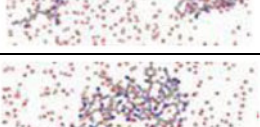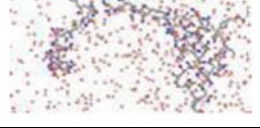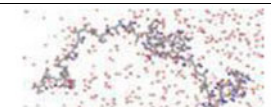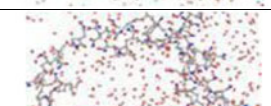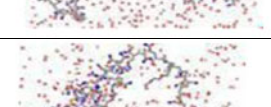
| Solution model | Molecule shape | Snapshot of mean conformation from simulations | $I_{NaCl}$ (mol/kg) | $N_{NaCl}$ | $V_{cell}$ (nm³) | $\rho_{NaCl}(10^{-3})$ (g·cm⁻³) | $\rho_{H2O}$ (g·cm⁻³) | $\rho_P$ (g·cm⁻³) | $L_{ef}$ (nm) | $\Lambda^*$ |
|---|---|---|---|---|---|---|---|---|---|---|
| HM-HPAM2 | Bent spheroid | | 0 | 0 | 59.8 | 0 | 1 | 0.21 | 4.0 | 10.5 |
| | | | 2.78×10-2 | 1 | 59.8 | 1.6 | 1 | 0.21 | 3.6 | 8.9 |
| | | | 0.11 | 4 | 59.8 | 6.5 | 1 | 0.21 | 3.2 | 7.9 |
| | | | 0.19 | 7 | 59.8 | 11.4 | 1 | 0.21 | 2.8 | 7.1 |
| | | | 0.28 | 10 | 59.8 | 16.5 | 1 | 0.21 | 2.7 | 7.0 |
| HM-PAM2 | Bent spheroid | | 0 | 0 | 59.8 | 0 | 1 | 0.21 | 2.4 | 5.3 |
| | | | 0.03 | 1 | 59.8 | 1.6 | 1 | 0.21 | 2.3 | 5.2 |
| | | | 0.11 | 4 | 59.8 | 6.5 | 1 | 0.21 | 2.2 | 5.1 |
| | | | 0.19 | 7 | 59.8 | 11.4 | 1 | 0.21 | 2.2 | 5.1 |
| | | | 0.28 | 10 | 59.8 | 16.5 | 1 | 0.21 | 2.2 | 5.1 |

**Table 3** Parameters for HM-HPAM3 and HM-PAM3 solution models at 298 K

| Solution model | Molecule shape | Snapshot of mean conformation from simulations | $I_{NaCl}$ (mol/kg) | $N_{NaCl}$ | $V_{cell}$ (nm$^3$) | $\rho_{NaCl}(10^{-3})$ (g·cm$^{-3}$) | $\rho_{H2O}$ (g·cm$^{-3}$) | $\rho_P$ (g·cm$^{-3}$) | $L_{ef}$ (nm) | $\Lambda^*$ |
|---|---|---|---|---|---|---|---|---|---|---|
| | |  | 0 | 0 | 59.8 | 0 | 1 | 0.22 | 4.5 | 11.8 |
| | |  | 0.03 | 1 | 59.8 | 1.6 | 1 | 0.22 | 4.1 | 10.7 |
| HM-HPAM3 |  Bent spheroid |  | 0.11 | 4 | 59.8 | 6.5 | 1 | 0.22 | 3.6 | 9.42 |
| | |  | 0.19 | 7 | 59.8 | 11.4 | 1 | 0.22 | 3.3 | 8.63 |
| | |  | 0.28 | 10 | 59.8 | 16.5 | 1 | 0.22 | 3.2 | 8.37 |
| | |  | 0 | 0 | 59.8 | 0 | 1 | 0.22 | 2.7 | 5.63 |
| HM-PAM3 |  Bent spheroid |  | 0.03 | 1 | 59.8 | 1.6 | 1 | 0.22 | 2.6 | 5.45 |
| | |  | 0.11 | 4 | 59.8 | 6.5 | 1 | 0.22 | 2.5 | 5.45 |
| | |  | 0.19 | 7 | 59.8 | 11.4 | 1 | 0.22 | 2.5 | 5.45 |
| | |  | 0.28 | 10 | 59.8 | 16.5 | 1 | 0.22 | 2.5 | 5.45 |

$\lambda^*$——see part 3 and ref. [28]

$I_{NaCl}$— ionic strength of the dilute solution; $N_{NaCl}$—the number of NaCl molecule; $V_{cell}$—the volume for cubic cell; $\rho_{NaCl}$— the density of NaCl

$\rho_{H2O}$—the density of $H_2O$; $\rho_P$—the density of HM- PAMs or HM- HPAMs

$L_{ef}$ — the effective length parameter or $2\,l/\pi$

The intrinsic viscosity

In this work, several dynamic properties of the modified poly-acrylamide in a dilute aqueous solution are investigated as follows, which can mirror salt concentrations on the structures of HM-PAM and HM-HPAM. In dilute solution, the intrinsic viscosity has been used to study the hydrodynamic volume of polymer chains and the interaction between polymer chains and solvent or between different polymer chains [30]. As reported

the intrinsic viscosity is greatly dependent on the salt concentration [31].

*The effective length parameter ($L_{ef}$)*

Tables 1, 2 and 3 presents examples of snapshots collected during simulations. Snapshots of the equilibrated HM-PAM/HM-HPAM chain configurations are shown in tables. For sake of convenience we have introduced here the effective

Fig. 4 Radius of gyration for HM-PAM (**a**) and radius of gyration for HM-HPAM (**b**) in different ionic strength solutions
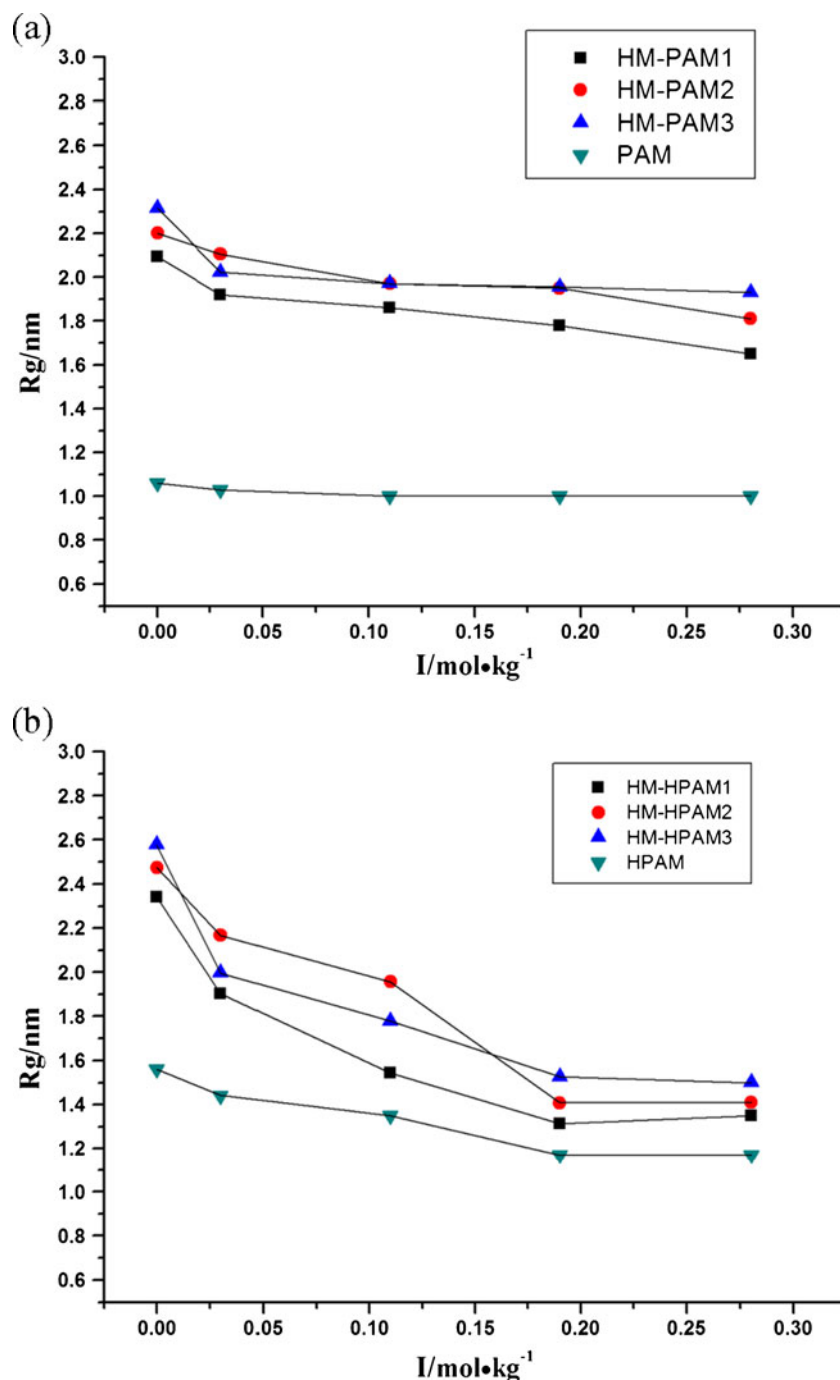
**Fig. 5** hydrodynamic radius for HM-PAM (**a**) and hydrodynamic radius for HM-HPAM (**b**) in different ionic strength solutions
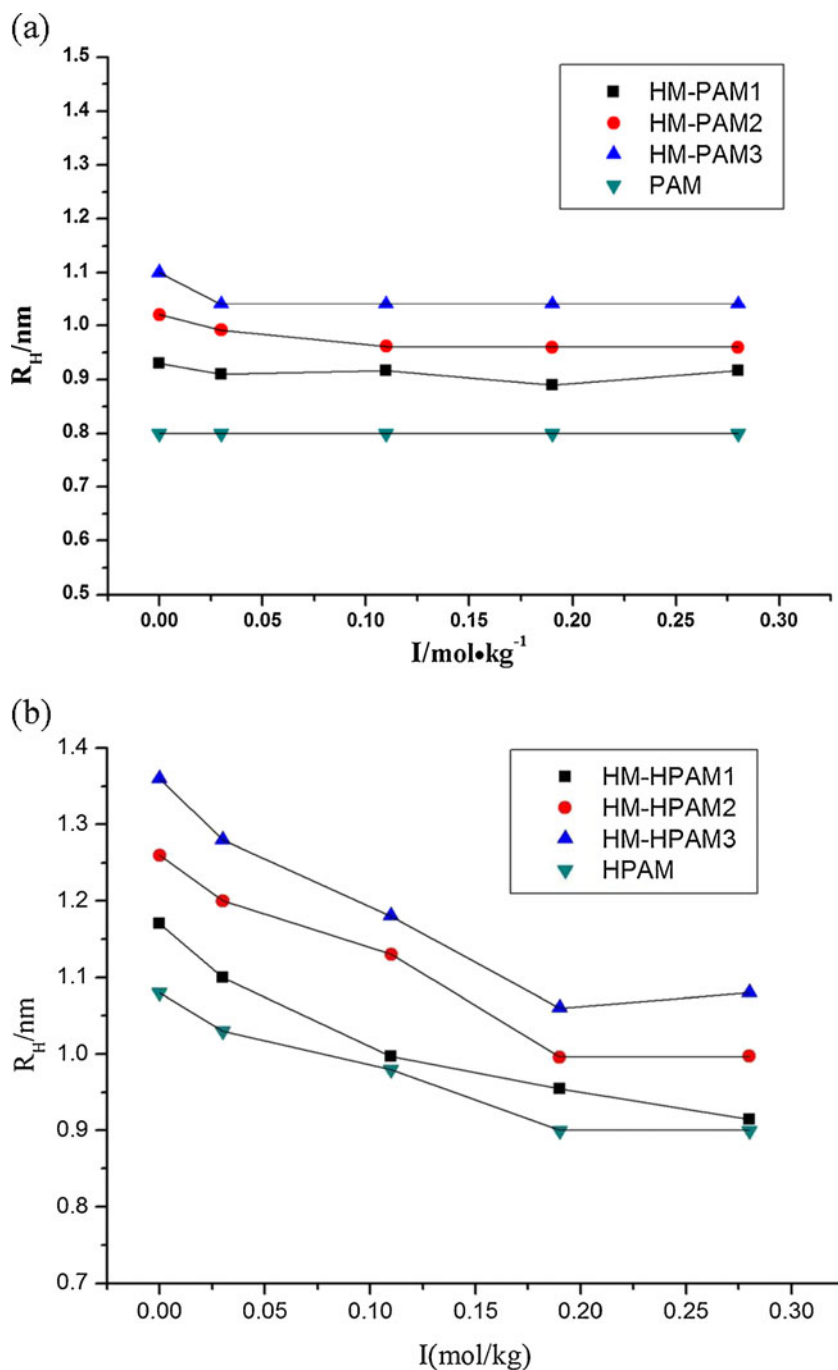


length parameter $L_{ef}$ which can be a useful measure of molecule dimensions if it assumes an elongated shape to take place of $2\,l/\pi$. That parameter also facilitates the interpretation of dynamic viscosity measurements in terms of the hydrodynamic theory. The effective length was calculated as a value of the distance between the surfaces of two outermost atoms of the molecule averaged at the fluctuating equilibrium state by the radial distribution function $g(r)$ [28]. The radial distribution function $g(r)$ can be used to measure either one or two sets of atoms via [10, 32, 33].

$$g(r) = \frac{1}{N}\left\langle \sum_{i=1}^{N}\sum_{j\neq 1}^{N}\delta(r - r_{ij})\right\rangle, \qquad (2)$$

$r_{ij}$ is the distance between a pair of atoms or centroids. In the case of a single set, the function is computed for all pairs of atoms or centroids in the set which are closer than the cutoff value. With two sets, the function is calculated for all pairs of atoms or centroids within each isolated set, as well as for all pairs containing one atom or centroid from each set, ignoring all pairs separated by distances greater than the cutoff.

**Fig. 6** Radius of gyration ($a_1$ and $a_2$), hydrodynamic radius ($b_1$ and $b_2$) and intrinsic viscosity ($c_1$ and $c_2$) vs ionic strength ($I_{NaCl}$) for HM-PAM1 and HM-HPAM1 solution models at 298 K
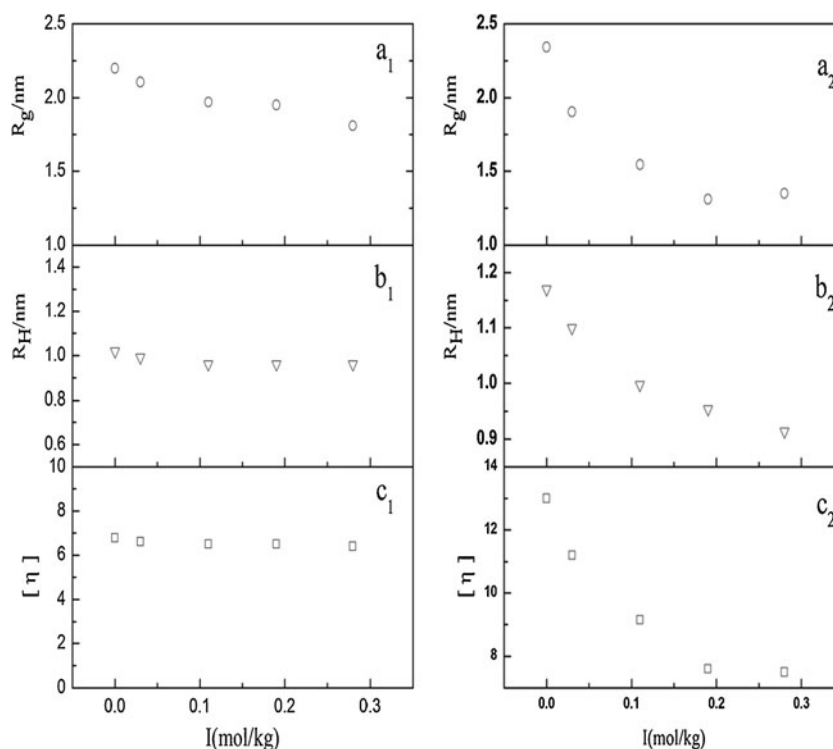


Table 3 for the HM-HPAM3, 25 % ionization degree indicate that the molecule shape assumes an extended, worm-like shape characterized by the average effective length $L_{ef}$=4.5 nm without addition of NaCl ($I$=0 mol/kg). For increasing ionic strength the contour is decreased because of the folding of the molecule, becoming 4.1 nm for $I$=$3\times10^{-2}$ mol/kg, 3.6 nm for $I$=0.11 mol/kg, 3.3 nm for $I$=0.19 mol/kg, and 3.2 nm for $I$=0.28 mol/kg. HM-HPAM1 and HM-HPAM2 have the same tendency. A similar behavior was predicted in the simulations of Adamczyk [28, 29] who studied conformations poly (allylamine hydrochloride) in electrolyte solutions. However, the average effective length ($L_{ef}$) increases one by one from HM-HPAM1/HM-PAM1 to HM-HPAM3/HM-PAM3 with the same ionic strength. The average effective length of HM-PAM has no significant change with increasing ionic strength and is lower than the values for HM-HPAM. For lower ionic strength, the polyelectrolyte chain becomes more extended, but for the $I$=0.19 mol/kg and $I$=0.28 mol/kg, the mean conformations of HM-HPAM have not shrunk any longer and the average effective lengths ($L_{ef}$) of HM-HPAM change very little, which agreed with the experimental results very well. Even for the highest ionic strength 0.28 mol/kg, the polyelectrolyte chain did not collapse and still keep bent spheroid.

*The radius of gyration ($R_g$) and the hydrodynamic radius ($R_H$)*

The radius of gyration $R_g(s)$ represents the molecular size of the polymer explored in this work, which is defined as the root mean square distance of the atoms in the molecule from their common center of mass, that is [10, 11, 34],

$$s^2 = \frac{\sum_{i=1}^{N} m_i s_i^2}{\sum_{i=1}^{N} m_i}, \qquad (3)$$

$s_i$ denotes the distance of atom $i$ from the center of mass and $N$ denotes the total number of atoms in the above expression. The radius of gyration $R_g$ for HM-PAM/HM-HPAM molecules were obtained by MD dynamic as show in Fig. 4. $R_g$ for HM-HPAM decreases gradually with increasing ionic strength and has no significant change with increasing ionic strength for HM-PAM, the tendency of $R_g$ was consistent with the effective length ($L_{ef}$) because the radius of gyration $R_g$ ($s$) represents the molecular size of the polymer explored in this work. The theoretical values of $R_H$ for various molecule shapes can be calculated from Eq. 1. The variation tendency of the $R_H$ was in accordance with $L_{ef}$ and $Rg$ as show in Fig. 5.

In addition, the hydrodynamic radius and the radius of gyration of a polymeric molecule in a solvent used to predict an approximation of the intrinsic viscosity via [33, 35]

$$[\eta] = \frac{6^{3/2} \Phi R_g^3}{M_w} \qquad (4)$$

$$[\eta] = 2.5 \frac{\frac{4}{3}\pi R_H^3 d N_A}{M_w}, \qquad (5)$$

Fig. 7 Radius of gyration ($a_1$ and $a_2$), hydrodynamic radius ($b_1$ and $b_2$), and intrinsic viscosity ($c_1$ and $c_2$) vs ionic strength ($I_{NaCl}$) for HM-PAM2 and HM-HPAM2 solution models at 298 K
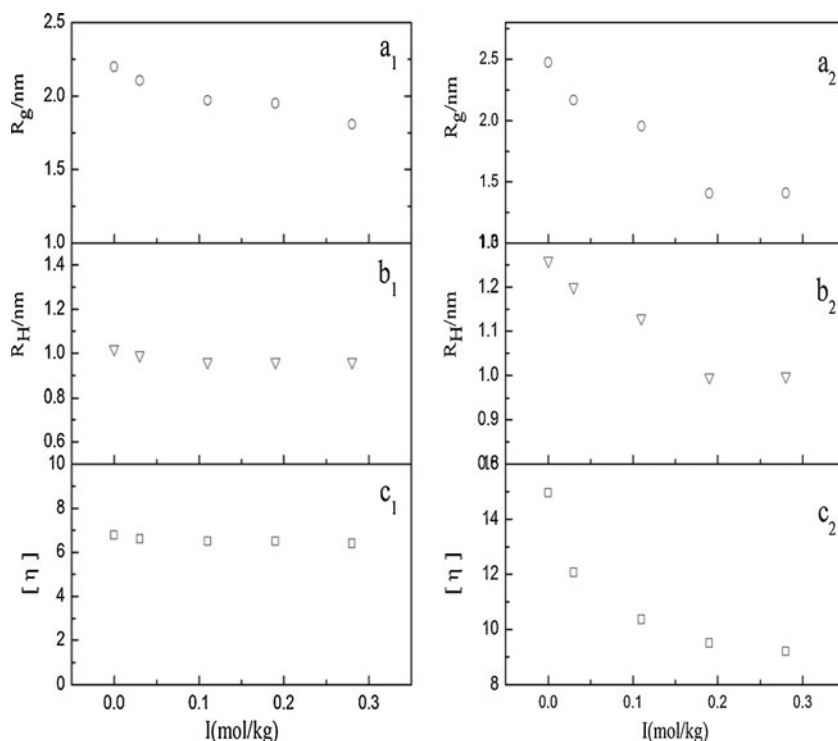


with $d$ the specific gravity of the solute, $N_A$ the Avogadro number, $M_w$ the molecular weight, and $\Phi$ the value reflecting the solvent quality [36]. According to Eq. 5, it is clear that the intrinsic viscosity is affected only by $R_H$ and proportional to $R_H^3$. While for Eq. 4, the intrinsic viscosity is determined by both $R_g^3$ and $\Phi$.

We can investigate $R_H$ for HM-HPAM or HM-PAM the change trends of which reflect the trends of intrinsic viscosity in the polymer solutions with different ionic strength in the MD simulations. Simultaneously, $R_g$ for HM-HPAM or HM-PAM can be gained using MD simulations to explore solvation power of the polymer under different ionic
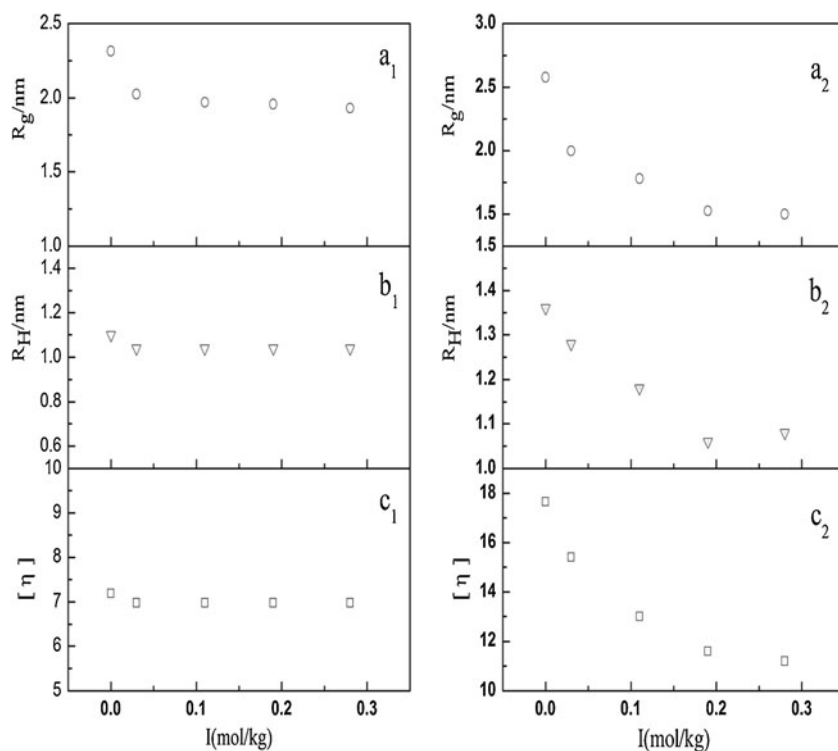
Fig. 8 Radius of gyration ($a_1$ and $a_2$), hydrodynamic radius ($b_1$ and $b_2$), and intrinsic viscosity ($c_1$ and $c_2$) vs ionic strength ($I_{NaCl}$) for HM-PAM3 and HM-HPAM3 solution models at 298 K

strength. In Figs. 6a, b, c, 7 a, b, c, and 8 a, b, c the $R_g$, $R_H$ and [$\eta$] for HM-HPAM or HM-PAM vs ionic strength are shown. It is clear that the trends of the [$\eta$] changes with increasing ionic strength are in good agreement with the $R_g$ and $R_H$.

So we can use $R_g$ and $R_H$ to predict [$\eta$] changes for HM-HPAM or HM-PAM solutions with different ionic strength as Eqs. 4 and 5 shown.

*The effect of ionic strength on the intrinsic viscosity*

Figure 4 shows the influence of ionic strength on intrinsic viscosities of the HM-PAM1 and HM-HPAM1 solution. With the ionic strength increasing, the intrinsic viscosity of the HM-HPAM1 decreases and the HM-PAM1 has no significant change and the same tendency as HM-HPAM2/HM-PAM2 and HM-HPAM3/HM-PAM3.

However, compared to PAM (HPAM) [15, 16] which has been studied by our previous work, HM-PAM (HM-HPAM) has a high intrinsic viscosity. The reason is interchain associations of the hydrophobe units, which are dispersed along the polyacrylamide backbone, lead to solutions of high intrinsic viscosity at low concentrations and low shear rates [37]. However, the intrinsic viscosity increases gradually from HM-HPAM1/HM-PAM1 to HM-HPAM3/HM-PAM3. A possible reason is that the effect of steric hindrance is increased gradually from monomer-1 to monomer-3 which enhances the impact of the interchain associations.

The HM-HPAM backbone consists of 74 % aminocarbonyl groups ($-CONH_2$) and 24 % carboxylate groups ($-COO^-$) and 4 % other comonomers. When the HM-HPAM is dissolved in deionized water, the HM-HPAM macromolecule with the carboxylate groups ($-COO^-$) can form electrical double layer and thick hydration film, which can pack more $H_2O$ molecules. Thus the HM-HPAM backbone will extend and have larger hydrodynamic volume, and accordingly the viscosity of solution will be higher than the HM-PAM [37]. The NaCl added to the HM-HPAM solution can ionize $Na^+$. Because of very high electric field generated by these closely packed charges, a significant adsorption of couterions ($Na^+$) from the supporting electrolyte occurred during initial stages of simulations. This phenomenon often referred to in the literature as the counterion condensation (Maning-Oosawa condensation) [28] leads to a significant compensation of the nominal charge of HM-HPAM, which was reduced to a small fraction of its initial value. Besides, the effective length, radius of gyration, hydrodynamic radius, its shape and the characteristic linear dimensions of the molecule under various conditions were determined [28, 29]. As a result, the higher ionic strength of the solution is, the lower intrinsic viscosity is, but at the last, the intrinsic viscosity keeps a constant, which is in accordance with the experiment very well.

For HM-PAM, the intrinsic viscosity has no significant change with increasing the ionic strength and the intrinsic viscosity values is lower than the values for HM-HPAM as seen in Figs. 6, 7 and 8. This lies in absence of ionic groups in HM-PAM chain and leads to the effective length, radius of gyration, hydrodynamic radius has no significant change.

The salt tolerance

To investigate the salt tolerance of HM-HPAM, we define a parameter $D$ as the declined proportion of the intrinsic viscosity from $I=0$ mol/kg to $I=0.28$ mol/kg, for example, for HM-HPAM1, the expression about $D$ is following,

$$D_1 = \frac{[\eta]_{1,I=0mol/kg} - [\eta]_{1,I=0.28mol/kg}}{[\eta]_{1,I=0mol/kg}} \times 100\%, \qquad (6)$$

$[\eta]_I=0$ mol/kg represents the value of the intrinsic viscosity for $I=0$ mol/kg, $[\eta]_I=0.28$ mol/kg represents the value of the intrinsic viscosity for $I=0.28$ mol/kg. $D$ represents declined proportion of the intrinsic viscosity from $I=0$ mol/kg to $I=0.28$ mol/kg. So, we can calcu-
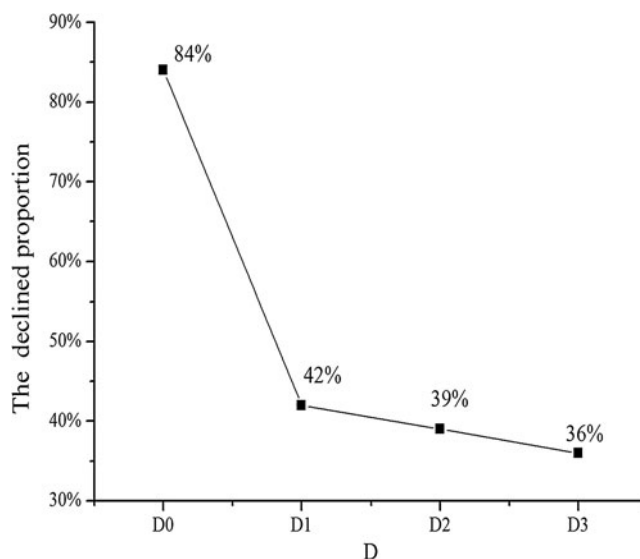


**Fig. 9** The declined proportion of the intrinsic viscosity for HPAM and HM-HPAM from $I=0$ mol/kg to $I=0.28$ mol/kg. $D$ represents declined proportion of the intrinsic viscosity from $I=0$ mol/kg to $I=0.28$ mol/kg

late the $D_0$, $D_1$, $D_2$, and $D_3$ through the expression above as shown in Fig. 9.

It can be seen from Fig. 9, the HM-HPAM has a stronger salt tolerance compared to HPAM and It can also be concluded that the salt tolerance increases gradually from HM-HPAM1 to HM-HPAM3. So the molecular design of modified polyacrylamide is good for the stronger salt tolerance. The monomers with the steric hindrance, which increases gradually from monomer-1 to monomer-3, would reduce the curliness of molecular chains and, consequently, improve the salt tolerance and the simulated results agree with the experimental results very well [6]. Such advantages provide the modified PAM with great potential in the enhanced oil recovery field.

The radial distribution function

$g(r)$ can give the appearance frequency of the atom [14]. the $O^-$ of the $-COO^-$ group of the HM-HPAM and $H_2O$ radial distribution function $g_{O^--H}(r)$ and the O of the $-CONH_2$ group of the HM-PAM and $H_2O$ radial distribution function $g_{O-H(r)}$ at different NaCl concentrations have been analyzed using molecular dynamics simulations. The results are shown in Figs. 10, 11 and 12. For HM-PAM, the value of $g_{O-H}(r)$ is zero when $r$ is less than 0.25 nm, it means that the $-CONH_2$ group cannot appear around the $H_2O$ molecule when their distance is below 0.25 nm; the peak of RDF appears when r is about 0.25 nm. And for HM-PAM1, the



Fig. 10 a RDF for O ($-CONH_2$) of HM-PAM2 and H ($H_2O$) in different ionic strength solutions. b RDF for $O^-$ ($-COO^-$) of HM-HPAM2 and H ($H_2O$) in different ionic strength solutions
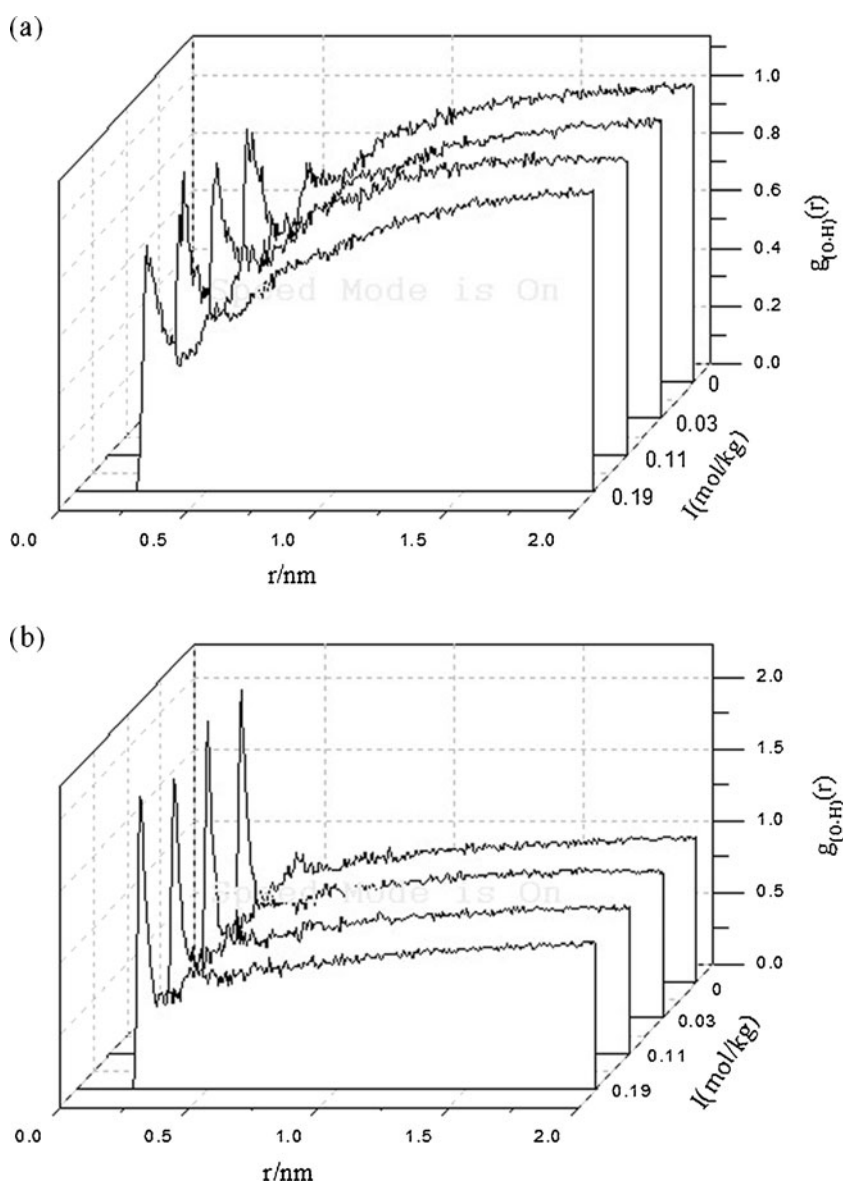
peak heights have no significant change, being 0.851, 0.75, 0.80 and 0.75 respectively. This implies the hydration of the O of the HM-PAM is very weak and not influenced basically by increasing ionic strength. HM-HPAM has the same results, but the peak heights are different; and for HM-HPAM1, it is about 2.2 for $I=0$ mol/kg and 1.2 for $I=0.19$ mol/kg, which means that the appearance frequency of $O^-$ around 0.25 nm of the $H_2O$ molecule is higher in $I=0$ mol/kg system than that in $I=0.19$ mol/kg system as seen in Fig. 10, which reduces the repulsion between $-COO^-$ groups of the HM-HPAM and increases the adsorption amounts of sodium ions at interface. The HM-HPAM2 and the HM-HPAM3 have the same situation as seen in Figs. 11

and 12. Consequently, $g(r)$ can explain a better thickening ability as well as poor salt tolerance for HM-HPAM compared to HM-PAM and the effect of NaCl on the hydration of the $-COO^-$ groups of the HM-HPAM from microscopic view.

## Conclusions

In this work, the modification of PAM/HPAM in a dilute aqueous solution by inducing three kinds of functional monomers was investigated by MD simulation with the PCFF force field. The characteristics of the HM-PAM/

Fig. 11 **a** RDF for O ($-CONH_2$) of HM-PAM2 and H ($H_2O$) in different ionic strength solutions. **b** RDF for $O^-$ ($-COO^-$) of HM-HPAM2 and H ($H_2O$) in different ionic strength solutions
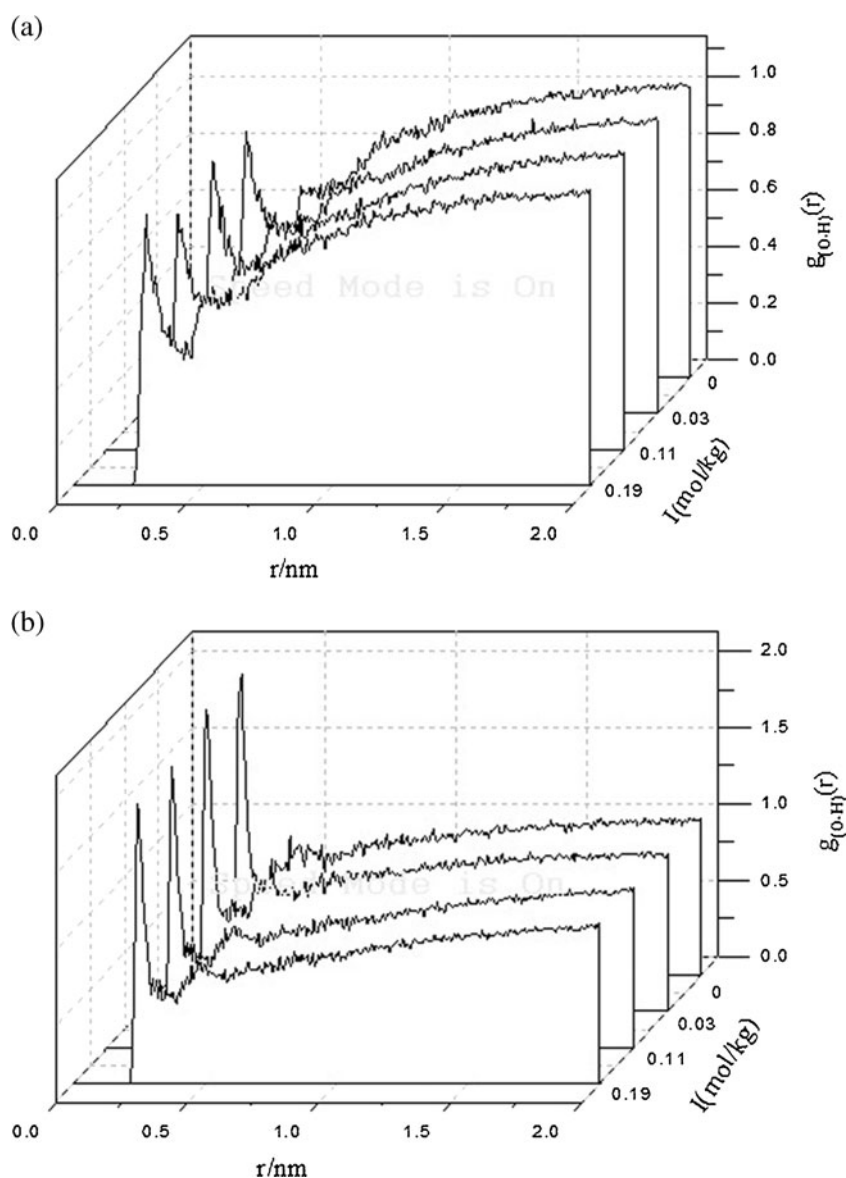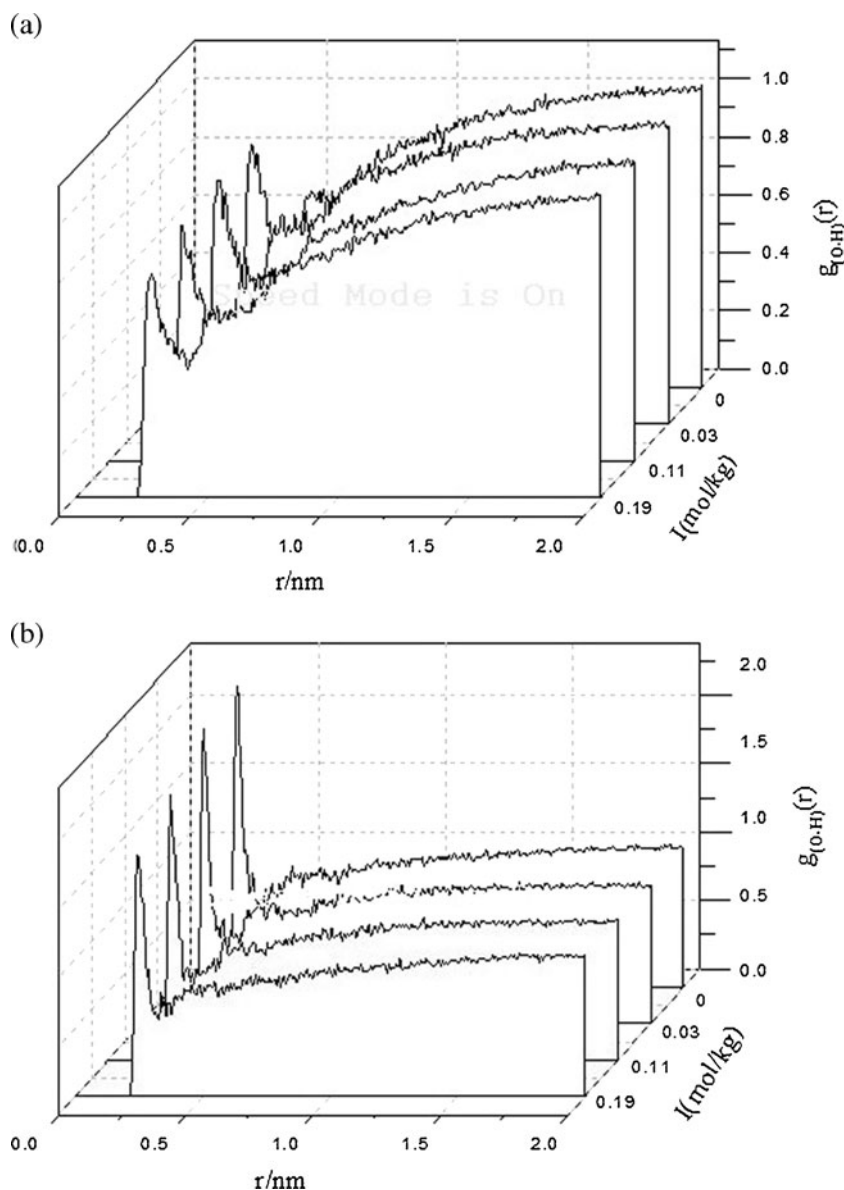
**Fig. 12 a** RDF for O
(−CONH₂) of HM-PAM3 and
H (H₂O) in different ionic
strength solutions. **b** RDF for
O⁻ (−COO⁻) of HM-HPAM3
and H (H₂O) in different ionic
strength solutions



HM-HPAM (such as the $R_g$, $R_H$ and RDF) have been studied to find the intrinsic relation between the microstructure of the polymer chain and the intrinsic viscosities. The simulation results show that the hydrodynamic radius, the radius of gyration and the intrinsic viscosity of the HM-HPAM chain decrease with the increasing NaCl concentration, and the hydrodynamic radius, the radius of gyration, the intrinsic viscosity of the HM-PAM chain have no significant change. Furthermore, compared to HPAM, the HM-HPAM has a stronger salt tolerance and the salt tolerance increases gradually from HM-HPAM1 to HM-HPAM3 because the monomers with steric hindrance would reduce the curliness of molecular chains and, consequently, improve the salt

tolerance. So, inducing the steric hindrance monomer into polymer will increase the salt tolerance of the polymer.

Ultimately, The RDF of the O⁻, which roots in the –COO⁻ group of the HM-HPAM with H₂O and the O, which roots in the –CONH₂ group of the HM-PAM with H₂O in a series of ionic strengths have been investigate by molecular dynamics simulation; which explains the effect of NaCl on the hydration of the –COO⁻ groups of the HM-HPAM from microscopic view.

# References

1. Unnithan MR, Vinod VP, Anirudhan TS (2004) Synthesis, characterization, and application as a Chromium(VI) adsorbent of amine-modified Polyacrylamide-grafted coconut coir. Ind Eng Chem Res 43:2247–2255. doi:10.1021/ie0302084

2. Yang MH (2001) The rheological behavior of polyacrylamide solution: II. Yield stress. Polym Test 20:635–642. doi:10.1016/S0142-9418(00)00084-2

3. Yang YJ, Grassl B, Billon G, Khoukh A, Francois J (2002) Effects of NaCl on steady rheological behaviour in aqueous solutions of hydrophobically modified polyacrylamide and its partially hydrolyzed analogues prepared by post-modification. Polym Int 51:939–947. doi:10.1002/pi.959

4. Zhang LH, Fang SW, Duan M, Wang FX, Zhang P, Zhang J, Chang DY (2011) Synthesis of star hydrophobically modified acrylamide copolymer and its dilute solution behavior in water. J Macromol Sci Part B Phys 50:153–163

5. Schuberth S, Münstedt H (2008) Transient elongational viscosities of aqueous polyacrylamide solutions measured with an optical rheometer. Rheol Acta 47:139–147. doi:10.1007/s00397-007-0221-8

6. Zhao YZ, Zhou JZ, Xu XH, Liu WB, Zhang JY, Fan MH, Wang J (2009) Synthesis and characterization of a series of modified polyacrylamide B. Colloid Polym Sci 287:237–241. doi:10.1007/s00396-008-1975-y

7. Shashkinaa YA, Zaroslova YD, Smirnova VA, Philippovaa OE, Khokhlova AR, Pryakhinab TA, Churochkina NA (2003) Hydrophobic aggregation in aqueous solutions of hydrophobically modified polyacrylamide in the vicinity of overlap concentration. Polymer 44:2289–2293. doi:10.1016/S0032-3861(03)00043-0

8. Gao BJ, Guo HP, Wang J, Zhang YP (2008) Preparation of hydrophobic association polyacrylamide in a new micellar copolymerization system and its hydrophobically associative property. Macromolecules 41:2890–2897. doi:10.1021/ma701967b

9. Gong LX, Zhang XF (2009) A new approach to the synthesis of hydrophobically associating polyacrylamide via the inverse miniemulsion polymerization in the presence of template. eXPRESS Polym Lett 3:778–787. doi:10.3144/expresspolymlett.2009.96

10. Dalakoglou GK, Karatasos K, Lyulin SV, Lyulin AV (2008) Brownian dynamics simulations of complexes of hyperbranched polymers with linear polyelectrolytes: effects of the strength of electrostatic interaction on static properties. Mater Sci Eng B 152:114–118. doi:10.1016/j.mseb.2008.06.012

11. Le TC, Todd BD, Daivis PJ, Uhlherr AJ (2009) Structural properties of hyperbranched polymers in the melt under shear via nonequilibrium molecular dynamics simulation. J Chem Phys 130:074901. doi:10.1063/1.3077006

12. Drew PM, Adolf DB (2005) Intrinsic viscosity of dendrimers via equilibrium molecular dynamics. Soft Matter 1:146–151. doi:10.1039/b501658d

13. Tung KL, Lu KT, Ruaan RC, Juin JY (2006) Molecular dynamics study of the effect of solvent types on the dynamic properties of polymer chains in solution. Desalination 192:380–390. doi:10.1016/j.desal.2005.07.043

14. Wu D, Feng YJ, Xu GY, Che YJ, Cao XR, Li YM (2007) Dilational rheological properties of gemini surfactant 1,2-ethanebis(dimethyl dodecyl ammonium bromide) at air/water interface. Colloids Surf A Physicochem Eng Aspects 299:117–123. doi:10.1016/j.colsurfa.2006.11.031

15. Liu YY, Chen PK, Luo JH, Zhou G, Jiang B (2010) Molecular simulation of dilute Polyacrylamide solutions. Acta Phys Chim Sin 26(X):001–009. doi:10.3866/PKU.WHXB20101110

16. Chen PK, Yao L, Luo JH, Liu YY, Zhou G, Jiang B (2012) Experimental and theoretical study of dilute polyacrylamide solutions: effect of salt concentration. J Mol Model. doi:10.1007/s00894-011-1332-9

17. Hansson T, Oostenbrink C, Van Gunsteren W (2002) Molecular dynamics simulations. Curr Opin Struct Biol 12:190–196. doi:10.1016/S0959-440X(02)00308-1

18. Bizzarri AR, Cannistraro S (2002) Molecular dynamics of water at the protein-solvent interface. J Phys Chem B 106:6617–6633. doi:10.1021/jp020100m

19. Bishop M, Kalos MH, Frisch HL (1979) Molecular dynamics of polymeric systems. J Chem Phys 70:1299–1304. doi:10.1063/1.437567

20. Fan CF, Cagin T, Chen ZM, Smith KA (1994) Molecular modeling of polycarbonate. 1. Force field, static structure, and mechanical properties. Macromolecules 27:2383–2391. doi:10.1021/ma00087a004

21. Pan R, Liu XK, Zhang AM, Gu Y (2007) Molecular simulation on structure–property relationship of polyimides with methylene spacing groups in biphenyl side chain. Comput Mater Sci 39:887–895. doi:10.1016/j.commatsci.2006.10.019

22. Fu CL, Ouyang WZ, Sun ZY, An LJ, Li HF, Tong Z (2009) Solvent size effect on the static and dynamic properties of polymer chains in athermal solvents. Polymer 50:5142–5148. doi:10.1016/j.polymer.2009.09.010

23. Andersen HC (1980) Molecular dynamics simulations at constant pressure and/or temperature. J Chem Phys 72:2384–2393. doi:10.1063/1.439486

24. Berendsen HJC, Postma JPM, Van Gunsteren WF, DiNola A, Haak JR (1984) Molecular dynamics with coupling to an external bath. J Chem Phys 81:3684–3690. doi:10.1063/1.448118

25. Sun H, Mumby SJ, Maple JR, Hagler AT (1994) An ab initio CFF93 all-atom force field for polycarbonates. J Am Chem Soc 116:2978–2987. doi:10.1021/ja00086a030

26. Yarovsky I, Evans E (2002) Computer simulation of structure and properties of crosslinked polymers: application to epoxy resins. Polymer 43:963–969. doi:10.1016/S0032-3861(01)00634-6

27. Soldera A (2002) Energetic analysis of the two PMMA chain tacticities and PMA through molecular dynamics simulations. Polymer 43:4269–4275. doi:10.1016/S0032-3861(02)00240-9

28. Adamczyk Z, Jachimska B, Jasiński T, Warszyński P, Wasilewska M (2009) Strucgture of poly(sodium 4-styrenesulfonate) (PSS) in electrolyte solutions: theoretical modeling and measurements. Colloids Surf A Physicochem Eng Aspects 343:96–103. doi:10.1016/j.colsurfa.2009.01.035

29. Adamczyk Z, Jachimska B, Jasiński T, Warszyński P (2010) Conformations of poly(allylamine hydrochloride) in electrolyte solutions: Experimental measurements and theoretical modeling. Colloids Surf A Physicochem Eng Aspect 355:7–15. doi:10.1016/j.colsurfa.2009.11.012

30. Cho J, Heuzey MC, Bégin A, Carreau PJ (2006) Viscoelastic properties of chitosan solutions: effect of concentration and ionic strength. J Food Eng 74:500–515. doi:10.1016/j.jfoodeng.2005.01.047

31. Ikeda Y, Beer M, Schmidt M, Huber K (1998) $Ca^{2+}$ and $Cu^{2+}$ induced conformational changes of sodium polymethacrylate in dilute aqueous solution. Macromolecules 31:728–733. doi:10.1021/ma970540p

32. Zhao W, Leroy F, Heggen B, Zahn S, Kirchner B, Balasubramanian S, Müller-Plathe F (2009) Are there stable lonpairs in room-temperature lonic liquids? Molecular dynamics simulations of 1-n-Butyl-3-methylimidazolium hexafluorophosphate. J Am Chem Soc 131:15825–15833. doi:10.1021/ja906337p

33. Aerts J (2000) Prediction of intrinsic viscosities of mixed hyperbranched-linear polymers. Comput Theor Polym Sci 10:73–81. doi:10.1016/S1089-3156(99)00035-5

34. Richards EL, Buzza DMA, Davies GR (2007) Monte carlo simulation of random branching in hyperbranched polymers. Macromolecules 40:2210–2218. doi:10.1021/ma0700126

35. Barré L, Simon S, Palermo T (2008) Solution properties of asphaltenes. Langmuir 24:3709–3717. doi:10.1021/la702611s

36. Kairn T, Daivis PJ, Matin ML, Snook IK (2004) Concentration dependence of viscometric properties of model short chain polymer solutions. Polymer 45:2453–2464. doi:10.1016/j.polymer.2003.12.034

37. Biggs S, Selb J, Candau F (1992) Effect of surfactant on the solution properties of Hydrophobically modified Polyacrylamide. Langmuir 8:838–847. doi:10.1021/la00039a01